Journal of Supramolecular Structure
and Cellular Biochemistry 17:213–221 (1981)
Cellular Recognition 403–411

Effects of Multiple Membranes on Measurements of Cell Surface Dynamics by Fluorescence Photobleaching

N.O. Petersen and W.B. McConnaughey

Chemistry Department, University of Western Ontario, London, Canada N6A 5B7 (N.O.P.) and Washington University Medical School, St. Louis, Missouri 63110 (W.B.M.)

Fluorescence photobleaching recovery curves on a pair of membranes at various separations were calculated from a detailed knowledge of the variation in relative illumination areas and intensities as well as in relative contributions to the collected intensity with membrane separation. The observed diffusion coefficients were found to be relatively insensitive to membrane separation in all cases. Only for membranes with very different mobilities are there significant differences in fractional recoveries. Systematic variations in fractional recoveries with cell thickness may be indicative of differential mobility in the apical and basal membranes.

Key words: fluorescence photobleaching, FPR, multiple membranes

Fluorescence microscopy techniques can serve to study dynamic events on surfaces of cells. One method, fluorescence photobleaching recovery (FPR) [1], is specifically designed to measure the diffusion rate of fluorescently labeled lipids or proteins in the cell membrane. The fluorescence from a small area on the cell surface illuminated with a laser beam focused by high-power microscope optics is continuously monitored. At a particular instant, a brief pulse of high-intensity laser illumination bleaches a portion of the fluorophores in the illuminated area and thereby decreases the observed fluorescence. The time course of recovery of fluorescence is governed by the dynamic events (eg, diffusion) that can exchange the bleached molecule for fluorescent ones. The extent to which the fluorescence recovers is a measure of the fraction of the fluorophores that are governed by the dynamic process. The detailed shape of the recovery curve depends on: (1) the transverse intensity profile of the laser beam (usually Gaussian), (2) the extent of bleaching and therefore the bleach intensity and duration, (3) the effective radius of the laser beam, and (4) the kinetics of the dynamic process (ie, the diffusion coefficient) [1].

Where possible, we have maintained the notation used in references [1] and [5].

Received April 6, 1981; accepted August 6, 1981.

0275-3723/81/1703-0213$03.00

The laser beam size varies along the direction of propagation and is focused at the membrane of interest. A second membrane would be out of focus and thus would be illuminated by a wider beam with weaker intensity and hence less bleaching. Consequently, the fluorescence recovery curve for such a second membrane could be significantly different and could affect the interpretation of the measurements. Typically, adherent cells vary in thickness from a fraction of one to several micrometers depending on the location on the cell body. In this report, we examine in some detail the possible consequences of the cell thickness variation for the FPR measurements.

MATERIALS AND METHODS

The photobleaching instrumentation used in these studies has been described elsewhere [2,3]. Beam measurements were performed by either translation of a reflective mirror surface through the beam [2,4] or by scan recovery measurements on thin (< 1 μm) samples of a fluorescent dye (3,3′dioctadecylindocarbocyanine [diI]) embedded in a Hardman epoxy and compressed between two microscope coverslips. The sample translator utilized in the experiments is based on a linear piezoelectric motor designed by WBM and has been described previously [2]. FPR curves were analyzed utilizing three parameter computer fitting routines written by S. Felder (Washington University Medical School).

RESULTS

Illumination and Collection Geometries

To estimate the effects of a second out-of-focus membrane on the FPR measurements, we needed to establish the beam radius at the focus, $w(z_o)$ and the divergence of the beam, ie, the variation in beam radius as a function of distance from the focal plane, $w(z-z_o)$. From this we can calculate the variation in intensity, $I(r, z-z_o)$, for a Gaussian beam, as:

$$I(r,z-z_o) = \frac{2P}{\pi\, w^2(z-z_o)}\, e^{-2r^2/w^2(z-z_o)}, \tag{1}$$

where P is the total laser power, and r is the position in the plane transverse to the laser. In addition, we needed to measure the collection efficiency function, E(z) [5], which is a measure of the fractional contribution of the fluorescence from the out-of-focus membrane to the total detected fluorescence.

Figure 1A shows the result of a large number of beam size measurements as a function of the distance from the focal plane. The scatter in these data arise from a combined uncertainty in the beam size measurement and the focusing position. The solid line is the curve predicted by the beam expansion formula [6]:

$$w^2(z-z_o) = w^2(z_o) + \left(\frac{\lambda(z-z_o)}{\pi\, w(z_o)}\right)^2, \tag{2}$$

with $\lambda = 528.7$ nm and $w(z_o) = 2.0$ μm. From this, we calculated the central intensity, $I(o,z-z_o)$, by equation 1 for $r=0$, shown in Figure 1B. This is an

important parameter for estimating the bleaching efficiency since the fraction bleached is [1]:

$$A(z-z_o) = F(0)/F(-) = 1 - K^{-1}(1-e^{-K}); \quad (3)$$

where K is a bleaching constant given by [1]:

$$K(z-z_o) = \alpha I'(0,z-z_o)T, \quad (4)$$

with T the duration of the bleach, α a first-order rate constant for bleaching, and $I'(0,z-z_o)$ the laser intensity during bleaching.

Figure 1C shows the normalized collection efficiency function, $E(z-z_o)$ appropriate to the experimental configuration (see figure legend) of Figure 1A. These data were obtained simply by measuring the total fluorescence from a thin fluorescent sample as a function of focusing position. The collected fluorescence is restricted by an image plane pinhole whose radius, s_o, is generally chosen to be approximately twice that of the beam size in the image plane (which is $w' = w(z_o) \times M$ with M being the total magnification). For the curves in Figure 1C obtained with a 40× objective*, $w(z_o) = 2.0$ μm, the beam image is 0.10 mm in radius and the image pinholes had 0.20 and 0.125 mm radii, respectively. Koppel et al [5] have shown that within certain approximations $E(z-z_o)$ is Lorentzian,

$$E(z-z_o) \cong \left[1 + \left(\frac{z-z_o}{\ell}\right)^2\right]^{-1}, \quad (5)$$

with ℓ being the half-width at half height. Accounting properly for the beam expansion (equ. [2]) ℓ becomes:

$$\ell = \left\{ \left[2s_o^2 + w^2(z_o)\right] / \tan^2 \alpha_o \right\}^{1/2}, \quad (6)$$

where α_o is the divergence angle of the objective ($\sin \alpha_o$ = numerical aperture/refractive index) [M. Schneider and W.W. Webb, personal communication.] The predicted values of ℓ are thus 17.6 μm and 12.0 μm for the curves in Figure 1C compared with 15.0 μm and 10.5 μm as measured. The measured curves are not Lorentzian for large values of $z-z_o$ reflecting the approximate nature of equation [5].

Effects on Diffusion

Having established the nature of the illumination geometry and measured the true collection efficiency, we calculated the expected fluorescence recovery curves [1] for a pair of identical membranes separated by a distance $z-z_o$. The resultant curves were then computer fit as if the data represented a single recovery component. The percent deviation of the best fit recovery time, τ_D, from the true

*There is a 1.25× auxillary lens in the Zeiss microscope so that M = 50 for a 40× objective.

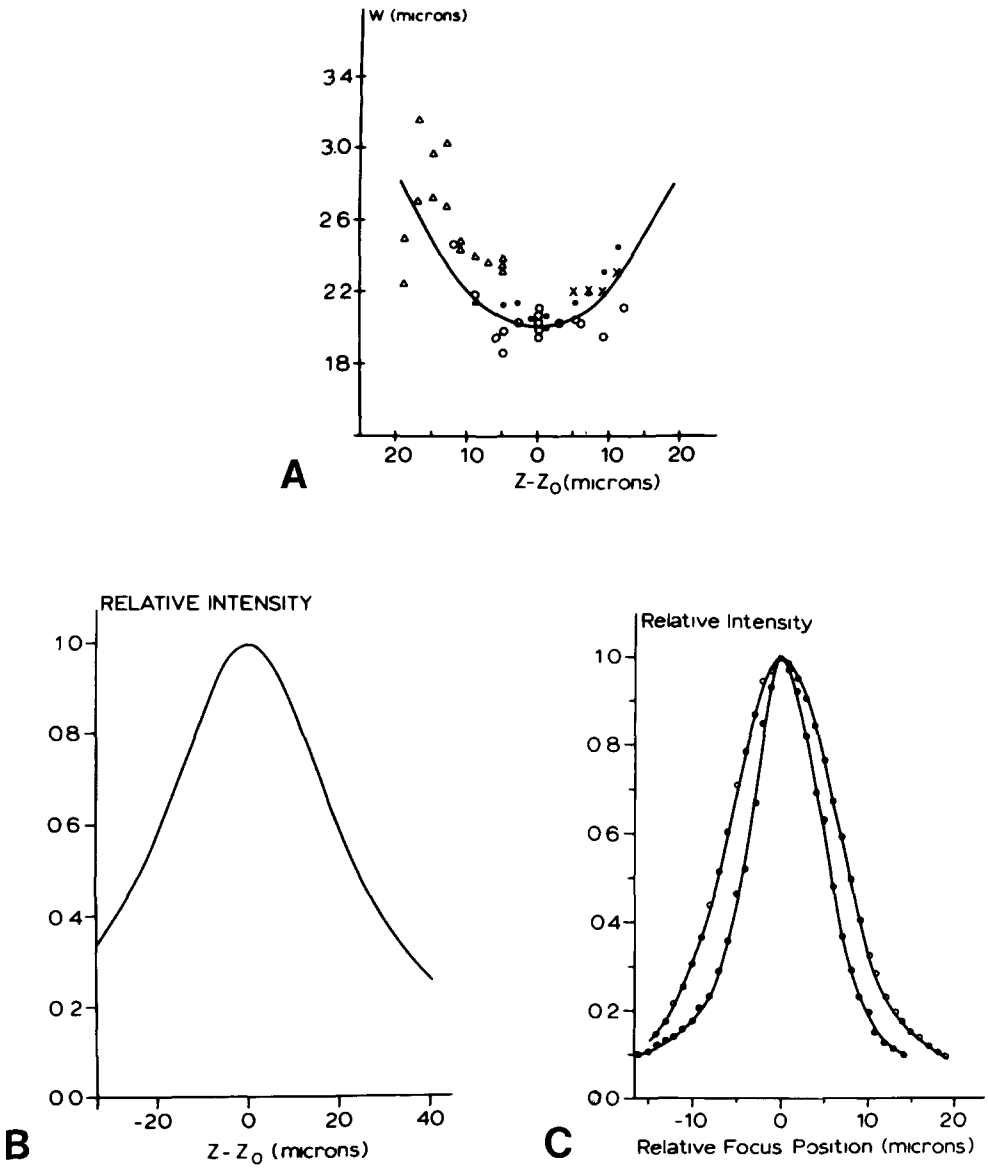

Fig. 1. A: Measured variation in beam radius as a function of the distance between the focal and object planes. Measurements for a 40× water immersion objective with both a reflective edge [△,X, ●] and a thin fluorescent sample [○] are included. The solid line is the predicted beam radius variation based on equation 2 with $w(z_0) = 2.0$ μm. B: Variation in the normalized central laser intensity, $I(0,z-z_0)/I(0,z_0)$ calculated from the beam radius change according to equations 1 and 2. C: Measured variation in normalized fluorescence intensity from a thin fluorescent film as a function of the distance between the focal and object planes. This corresponds to the collection efficiency function $E(z-z_0)$ described by Koppel et al [5]. The data shown are for a 40× water immersion objective with $w(z_0) =$ 2.0 μm and with image plane pinhole radii of 0.20 mm (○) and 0.125 mm (●), respectively. The full widths at half heights are 15.0 and 10.5 μm, respectively.

recovery time was then calculated as a function of membrane separation. For the geometry represented by Figure 1, the largest deviation of the fitted τ_D from the true τ_D was less than 6% and occurred over a range of separations between 5 and 15 μm. This is less than the usual experimental uncertainty of FPR experiments, and consequently, we expect very little effect from the cell thickness under these conditions. It is possible to focus the beam more sharply with the appropriate external lenses. Figure 2 shows the expected percent deviation in τ_D as a function of membrane separation for a 1.0 μm beam radius with a 40× objective and the $E(z-z_o)$ functions of Figure 1C. The deviations are still small (<25%) but are greatest at 6–8 μm, which is a typical cell thickness in the perinuclear region. Thus, measurements on different regions of a cell may introduce systematic variations in the measurements of as much as 25% resulting in a larger scatter than the technique is otherwise capable of providing.

It is possible to make measurements with large image pinholes or even without any. The depth of focus effects imposed by $E(z-z_o)$ then are absent. Nevertheless, $I(0, z-z_o)$ decreases as $z-z_o$ increases (see Figure 1B), which reduces the fraction bleached in the out-of-focus membrane and thus decreases its contribution to the measured recovery curve. Since $I(0, z-z_o)$ decreases less rapidly than $E(z-z_o)$ for small pinholes a larger pinhole will allow for a greater effect on τ_D. For $K \leq 2$, the measured τ_D is approximated well by a linear combination of the two contributing

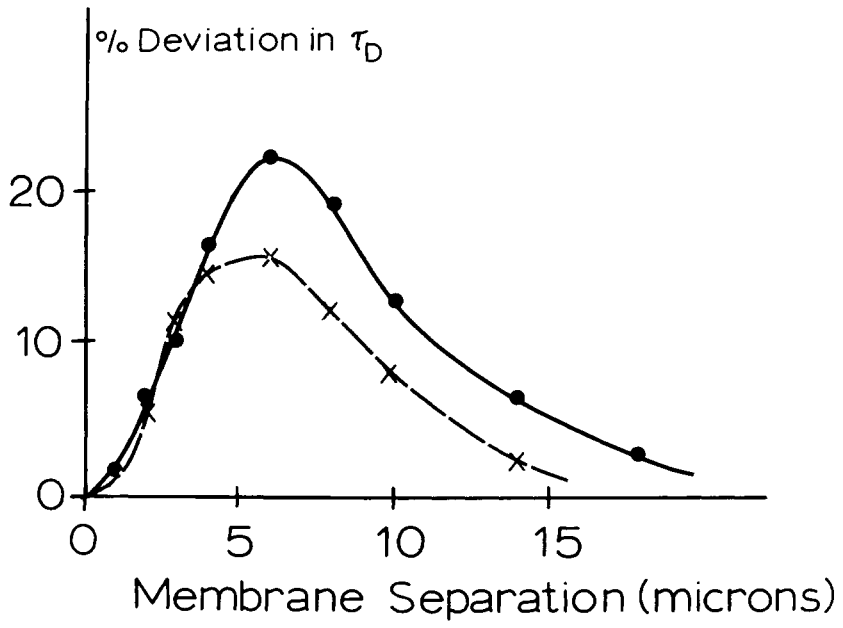

Fig. 2. The percent deviation in the fitted τ_D from the true τ_D for two identical membranes as a function of their separation. The curves illustrate the deviation expected for a 1.0 μm beam radius focused by a 40× objective given the collection efficiency functions of Figure 1C for 0.20 mm (○) and 0.125 mm (X) pinhole radii and using K = 2 (56% bleaching) on the focused membrane.

recovery times weighted by their respective recovery amplitudes. On this basis, we estimate the maximum effect on the out-of-focus membrane to be about 50% when $E(z-z_o)$ is not contributing to the depth of focus.

If the two membranes have different diffusion kinetics, more complex, but still small, effects can be expected. If the in-focus membrane exhibits mobility and the other membrane has totally immobile components there is no effect on τ_D of the second membrane. Conversely, if the out-of-focus membrane has mobile components while the in-focus membrane has none, then

$$D_T^{obs} = D_T \times \left(\frac{w^2(z_o)}{w^2(z-z_o)} \right) \tag{7}$$

When the diffusion coefficients are similar but the fractional recoveries differ, the effects on the observed diffusion coefficients are less than in the limiting cases. Thus if the in-focus membrane shows the greater fractional recovery, the effect of the second membrane is less than when the two membranes are identical. Conversely, if the out-of-focus membrane shows the greater fractional recovery, its effect is less than or in the limit equal to that given by equation 7. These results are summarized in Table I.

Effects on Fractional Recovery

The fractional recovery is a measure of the fraction of the fluorophores that are free to undergo diffusive motion and is defined [1] as:

$$F_R = \frac{F(\infty) - F(0)}{F(-) - F(0)}, \tag{8}$$

where, as in reference [1], $F(-)$, $F(0)$, and $F(\infty)$ are the fluorescence levels before, immediately following, and at long times after the bleach, respectively. It is easy to show that for two membranes (designated by the superscripts f and o for in-focus

TABLE 1. Summary of dual membrane effects on D_T and F_R

		Effect on D_T	Effect on F_R
I:	$D_T^F \cong D_T^O$ $F_R^F \cong F_R^O$	For 40 X/W w = 2 μM: <5% w = 1 μM: <25%	None
II:	$D_T^F \cong D_T^O$ $F_R^F \neq F_R^O$	Smaller than I if $F_R^F > F_R^O$ Smaller than IV if $F_R^F < F_R^O$	$F_R^{OBS} = \dfrac{A^F F_R^F + A^O E(z-z_o) F_R^O}{A^F + A^O E(z-z_o)}$
III:	$D_T^F >> D_T^O$ $(F_R^F >> F_R^O)$	None	$F_R^{OBS} = \dfrac{A^F}{A^F + A^O E(z-z_o)} F_R^F$
IV:	$D_T^F << D_T^O$ $(F_R^F << F_R^O)$	$D_T^{OBS} = D_T^O \left(\dfrac{w^2(z_o)}{w^2(z-z_o)} \right)$	$F_R^{OBS} = \dfrac{A^O E(z-z_o)}{A^F + A^O E(z-z_o)} F_R^O$

and out-of-focus respectively) separated by a distance $z-z_o$, the observed fractional recovery is:

$$F_R^{obs}(z-z_o) = \frac{A^f F_R^f + E(z-z_o)A^o F_R^o}{A^f + E(z-z_o)A^o}, \quad (9)$$

with A^f and A^o given by equation 3 and F_R^f and F_R^o designating the true fractional recovery in the respective membranes.

Clearly, if the membranes are identical, there is no effect of cell thickness on the observed fractional recovery. If the fractional recovery in one membrane is zero, the observed fractional recovery is strongly affected. Thus if $F_R^o = 0$:

$$F_R^{obs}(z-z_o) = \frac{A^f}{A^f + A^o E(z-z_o)} F_R^f = Q^o F_R^f \quad (10)$$

or conversely if $F_R^f = 0$:

$$F_R^{obs}(z-z_o) = \frac{A^o E(z-z_o)}{A^f + A^o E(z-z_o)} F_R^o = Q^o F_R^o \quad (11)$$

The factors $Q^f(z-z_o)$ and $Q^o(z-z_o)$ are plotted in Figure 3 as a function of membrane separation. Intermediate cases are obtained as the appropriate linear combinations of these ($F_R = Q^f F_R^f + Q^o F_R^o$). These results are summarized in Table I.

DISCUSSION

We have demonstrated that for the optical geometry employed in FPR instrumentation currently in use in our laboratory the laser illumination geometries and the collection efficiency functions conform closely to theoretical predictions [5,6]. We exploited these findings to calculate the effects on the FPR measurements of simultaneously illuminating and detecting fluorescence from two membranes at various separations as would be expected for adherent cells of varying thickness. The results are summarized in Table I. Four important conclusions emerge. First, the effects on the measured diffusion coefficients are small for all membrane separations and can be kept below 20%–25% deviation from the true value. This is because at small separations where the fluorescence contributions from both membranes are significant, the beam sizes are close so the fraction bleached, and the rates of recovery are similar for the two membranes. At larger separations where the beam sizes at the two membranes differ significantly, the contribution from the out-of-focus membrane to the total fluorescence is small. The maximal effect occurs at separations about equal to the half width, ℓ, of the collection efficiency function, $E(z-z_o)$. Second, the effects on the diffusion are at or slightly above the precision the instrumentation is capable of providing ($\cong$ 10%). Variations in cell thickness or shape might then be one source of the substantially larger scatter of the data frequently observed ($\cong$ 30%) [3]. Third, the effects on the measured fractional recoveries can be significant, only if the membranes behave differently. In the

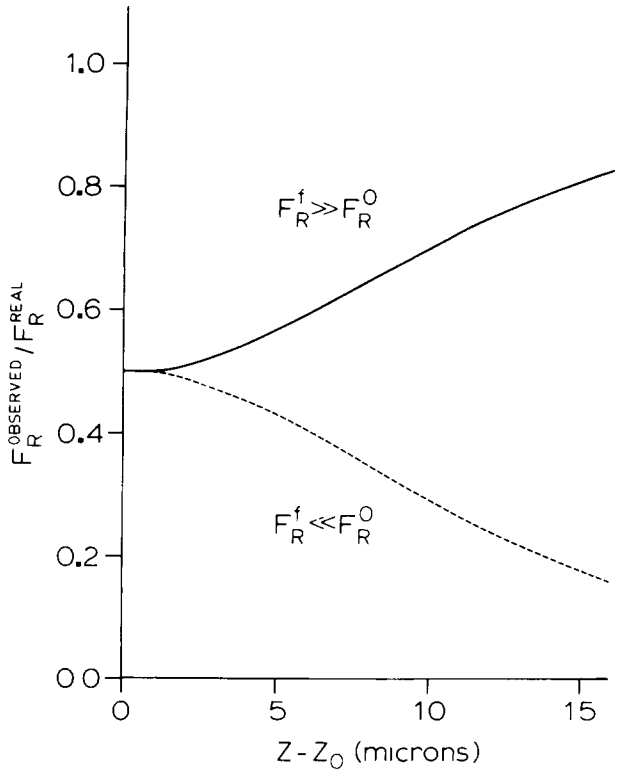

Fig. 3. Variation in the ratio of observed to real fractional recovery as a function of separation of two membranes with large differences in F_R values. The solid line corresponds to the case where the in-focus membrane exhibits much greater mobility. This curve is $Q^f(z-z_0)$. The broken line corresponds to the converse case where the out-of-focus membrane exhibits greater mobility. This curve is $Q^0(z-z_0)$.

extreme case where the out-of-focus membrane has only immobile (or very slowly diffusing) components, the maximal change in fractional recovery is from $\frac{1}{2}F_R^f$ in the thin regions to F_R^f in the very thick regions, ie, a twofold change.

Conversely, if the out-of-focus membrane has mobile components, but the in-focus membrane has only immobile components, the fractional recovery will change from a maximal value of 0.5 in the thin regions to 0 (or <0.1 in practice) in the thick regions. These findings provide an experimental test for differential mobilities in the two membranes of the cell. By consistently focusing on either of the two membranes (apical or basal surface) and measuring on many regions on the cell body, there should be trends of either larger or smaller fractional recoveries in the thin regions indicative of differential mobilities. In well-behaved systems, it might be possible to estimate the respective fractional recoveries for the two membranes, especially if the cell thickness can be estimated from the microscope focusing. Fourth, it is possible that the incomplete recovery frequently observed for proteins in cell membranes could arise from immobile fluorophores in the out-of-focus membrane, for example the basal surface, rather than from inherent mobility

restrictions. If so, the recovery should always be larger on the thicker regions of the cell. In the systems examined so far with this point in mind, no such systematic effects have been observed [Y. Henis, personal communication].

It is unlikely that cell morphology variations introduce large errors in the diffusion constant estimates obtained by fluorescence photobleaching recovery measurements, although increased scatter in the data may result. Since the fractional recovery is independent of cell thickness for identical membranes, the cell morphology as a general rule is not a parameter of concern in FPR experiments. However, substantial variations in the fractional recovery can result from cell morphology effects if there are intrinsic differences in the mobility between the basal and apical membranes. In favorable cases, it may be possible to explore the variation in fractional recovery with cell thickness to ascertain which membrane exhibits greater mobility.

ACKNOWLEDGMENTS

We gratefully acknowledge the help and support of Professor E.L. Elson in whose laboratory this work was done. We greatly appreciate the use of the fitting programs developed by S. Felder and thank M. Schneider and W.W. Webb for access to unpublished information. This work was supported by NIH General Medicine grants GM21661 and GM27160 to Dr. E.L. Elson. N.O.P. is currently a University of Western Ontario University Research Fellow.

REFERENCES

1. Axelrod D, Koppel DE, Schlessinger J, Elson EL, Webb WW: Biophys J 16:1055-1069, 1976.
2. Petersen NO, McConnaughey WB, Elson EL: Biophys J (submitted).
3. Henis YI, Elson EL: Proc Natl Acad Sci USA 78:1072-1076, 1981.
4. Suzaki Y, Tachibana A: Applied Optics 14:2809-2810, 1975.
5. Koppel DE, Axelrod D, Schlessinger J, Elson EL, Webb WW: Biophys J 16:1315-1329, 1976.
6. Kogelnik H: Bell System Technical J 44:455-494, 1965.